

pubs.acs.org/JACS Article

Cascade Synthesis of Fluorinated Spiroheterocyclic Scaffolding for Peptidic Macrobicycles

Angel Mendoza, Salvador J. Bernardino, Morris J. Dweck, Isabel Valencia, Declan Evans, Haowen Tian, William Lee, Yu Li, Kendall N. Houk, and Patrick G. Harran*



Cite This: J. Am. Chem. Soc. 2023, 145, 15888-15895



ACCESS I

Metrics & More

Article Recommendations

SI Supporting Information

ABSTRACT: Octafluorocyclopentene (OFCP) engages linear, unprotected peptides in polysubstitution cascades that generate complex fluorinated polycycles. The reactions occur in a single flask at 0–25 °C and require no catalysts or heavy metals. OFCP can directly polycyclize linear sequences using native functionality, or fluorospiroheterocyclic intermediates can be intercepted with exogenous nucleophiles. The latter tactic generates molecular hybrids composed of peptides, sugars, lipids, and heterocyclic

components. The platform can create stereoisomers of both single- and double-looped macrocycles. Calculations indicate that the latter can mimic diverse protein surface loops. Subsets of the molecules have low energy conformers that shield the polar surface area through intramolecular hydrogen bonding. A significant fraction of OFCP-derived macrocycles tested show moderate to high passive permeability in parallel artificial membrane permeability assays.

■ INTRODUCTION

Reaction processes that form multiple covalent bonds while creating new rings and stereocenters are inherently valuable in organic synthesis. They lead to the advancement of an overarching goal of the field, which is to enable syntheses of value-added products from abundant raw materials in the most direct manner possible. Reaction cascades have been used effectively for the synthesis of diverse carbocyclic and heterocyclic ring systems, using both catalytic and stoichiometric methods. 1,2 The typical objective is to streamline the assembly of molecules. However, multibond-forming processes can also manipulate the form and properties of preassembled structures. For example, we have developed reagents that can engage small peptides in successive ring-forming reactions to afford polycyclic derivatives. $^{3-11}$ In the example shown in Figure 1B, three consecutive operations imbed the core of the synthetic reagent 1 into unprotected WWY. Four new bonds (red) are formed between the oligomer and the scaffolding reagent, resulting in four new rings and three new stereocenters.8 Other methods to cyclize unprotected peptides using native functional groups (e.g., Figure 1A) achieve less bonding with the scaffold and install fewer conformational constraints. 12-16 Using 1 and related reagents, it is possible to convert machine-made oligomers systematically into stable composite macrocycles having diverse shapes and improved pharmacological properties.17

The scaffolding imparted by residual 1 (colored blue in 2) is hydrophobic. It was of interest to develop methods that could install scaffolding having polar elements and the potential for transannular hydrogen bonding. Here, we describe new polysubstitution cascades that achieve this outcome. The reactions modify linear, unprotected peptides in a single flask at room temperature. They require no catalysts or heavy metals, and they generate a wealth of previously unknown heterocyclic ring systems with tunable properties.

Electron-deficient aryl fluorides participate in nucleophilic ipso substitution (S_NAr) reactions. Sanger's method for Nterminal peptide sequencing is a seminal example.¹⁸ More heavily fluorinated aromatics such as hexafluorobenzene can engage two nucleophiles successively at ring positions 1 and 4. The reaction is efficient with sulfur nucleophiles and has been used to generate macrocyclic peptides via cysteine "stapling". 13 Polysubstitutions become possible when using perfluorinated cycloalkenes. For example, commercial octafluorocyclopentene (OFCP) reacts with simple nucleophiles at both its vinyl positions and subsequently at its allylic positions to afford adducts having up to six fluorine atoms replaced. 19 We have discovered how to translate this incremental electrophilicity of OFCP into relative rate-controlled substitution cascades. Using peptides as polynucleophilic partners, OFCP generates multicyclic products from linear precursors in a sequence-dependent manner.

Received: March 25, 2023 Published: July 13, 2023





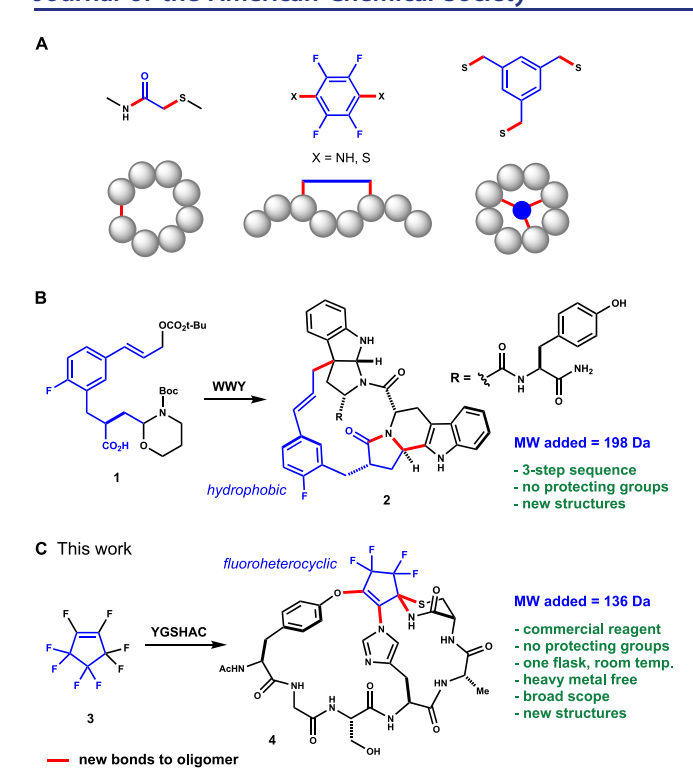


Figure 1. Cyclizations of linear, unprotected peptides. (A) Common side chain engagements using native functional groups (refs 12, 15). (B) Previous work—sequenced main chain and side chain reactions using multicontact scaffolding. (C) New discovery: relative rate-controlled polysubstitution cascades using perfluorocyclopentene.

We show how fluorinated thiazaspirodecenone intermediates can be intercepted to generate novel glycoconjugates, functionalization products, and macrobicyclic composites using molecular inserts. We study the molecular properties of end products and computationally probe how fluorospirocyclic scaffolding can generate new structural mimics of major loop types observed at protein contact surfaces in the Protein Data Bank.

■ RESULTS AND DISCUSSION

Linear peptides having three proximal nucleophilic residues react with OFCP (1.5 equiv, 25 °C, Et₃N, DMF) according to the progression shown in Figure 2A. Two successive vinylic substitutions occur rapidly ($k_{\rm rel}$ for Ser/Tyr/His/Cys ~ 1:30:45:1000) to afford macrocycles 6.20 DFT calculations have been performed to elaborate details of the mechanism. The potent electrophilicity of OFCP is related to the high stabilization of anionic intermediates by negative hyperconjugation. This is reflected, for example, in the highly delocalized HOMO calculated for the intermediate formed in the model reaction of ethyl mercaptide with OFCP (Figure 2B). Fluoride loss from this intermediate is calculated to have a very low barrier (see the SI). Excess OFCP (b.p. = 27 °C@1 atm) is removed from 6 in vacuo and the residue is redissolved in a DMF/THF solution containing excess Cs₂CO₃ or KOSiMe₂. This initiates spirocyclization via Sn2' displacement of a third fluorine atom (when Nu³ is a C-terminal carboxamide) to afford a new vinyl fluoride that is captured by a fourth competent nucleophile to give polycycles 8. Compounds 8 are stable, soluble, and purified using standard chromatographic techniques. Ac-YNCTFC-NH₂ reacts with

OFCP at its two cysteine residues within minutes at 25 °C. Subsequent Cs₂CO₃ treatment installs the thiazaspirodecenone motif while forming a new vinyl fluoride that then captures the N-terminal tyrosine residue to afford 9 in 41% isolated yield (Figure 2C). By initiating reaction cascades at a C-terminal cysteine amide, it is possible to synthesize a range of macrobicyclic structures that are bridged by sulfide and imidazole linkages. There is flexibility in ring size on either side of the bridging residue and, in the case of the histidine derivative 4, the bridge position epimer 13 can be prepared readily. Diastereoselectivity at the newly formed spiro center is high (>10:1) across the series. Products show sharp, wellresolved ¹H NMR spectra at ambient temperature. By repositioning the cysteinyl amide off of a glutamate or aspartate side chain, it is possible to initiate alternate macrobicyclization cascades. For example, the branched peptide Ac-YGAE(C)H-NMe2 affords the striking, doublelooped polycycle 16 when reacted successively with OFCP and KOSiMe₃. To our knowledge, each of the ring systems shown in Figure 2C are without a precedent in the literature.

It is possible to isolate and characterize vinyl fluorides 7. As shown in Figure 3A, treatment of Ac-CWSC-NH₂ with OFCP followed by KOSiMe₃ affords the spiro tricyclic compound 17 (35%, >10:1 d.r.). Under identical conditions, the same sequence containing D-cysteine affords epimeric macrocycle 25 (Figure 3B), while its homo cysteine variant affords spiro thiazepinone 26 in good yield and diastereoselectivity (>10:1 d.r.). Smaller ring analogs are also accessible. Omitting the tryptophan residue results in the formation of the spiro tricyclic substance 24.

The vinyl fluoride in 17 can be intercepted in bimolecular reactions to give a variety of substituted and homologated derivatives. It reacts with commercial β -D-thioglucose sodium salt within minutes at 25 °C to afford the unprotected glycoconjugate 19 in near quantitative yield. By varying the peptide sequence and the thioglycoside used, amalgamations with OFCP could generate a new class of glycosylated cyclic peptidomimetics. Compound 17 also reacts with a coniferyl alcohol derivative to afford 20. The cinnamyl carbonate in 20 provides means to form an additional large ring via electrophilic capture of amines, carboxylates, imidazoles and pi basic aromatic residues (e.g., see Figure 1B).³⁻¹¹ Azidation of 17 with NaN3 in DMF provides vinyl azide 21 in >95% yield. This molecule participates in Sharpless/Huisgen "click" cycloadditions with terminal alkynes. Stirring 21 with 1.0 equiv of propargyl alcohol in the presence of a phenylenediamine ligated Cu^{II} catalyst affords triazole 23 in 75% yield.²¹ Alternatively, azide 21 can be hydrogenolyzed to afford β thio enamine 22. This molecule can be purified without hydrolysis. Its amino group strongly resists acylation, even with Ac₂O/DMAP. Proximal fluorination attenuates its nucleophilicity. In fact, inductive deactivation appears to have an impact on the stability of these structures in general. For example, 13 and 24 are stable (<5% loss by HPLC analysis) in aqueous buffer of varying pH for extended periods of time (72 h at pH 4.5, 7.0, and 10.0, 25 $^{\circ}$ C). In addition, both compounds were stable to superstoichiometric amounts of N-chlorosuccinimide (NCS) and 30% aq. H_2O_2 (2.0 equiv oxidant, pH 4.5 buffer/ CH₃CN, 25 °C) over 72 h. The alkene, the thioaminoketal, the imidazole, and the sulfur atoms were unaffected in these experiments. For comparison, the disulfide derived from hexapeptide HFCASC (\$30, the linear precursor to 10)

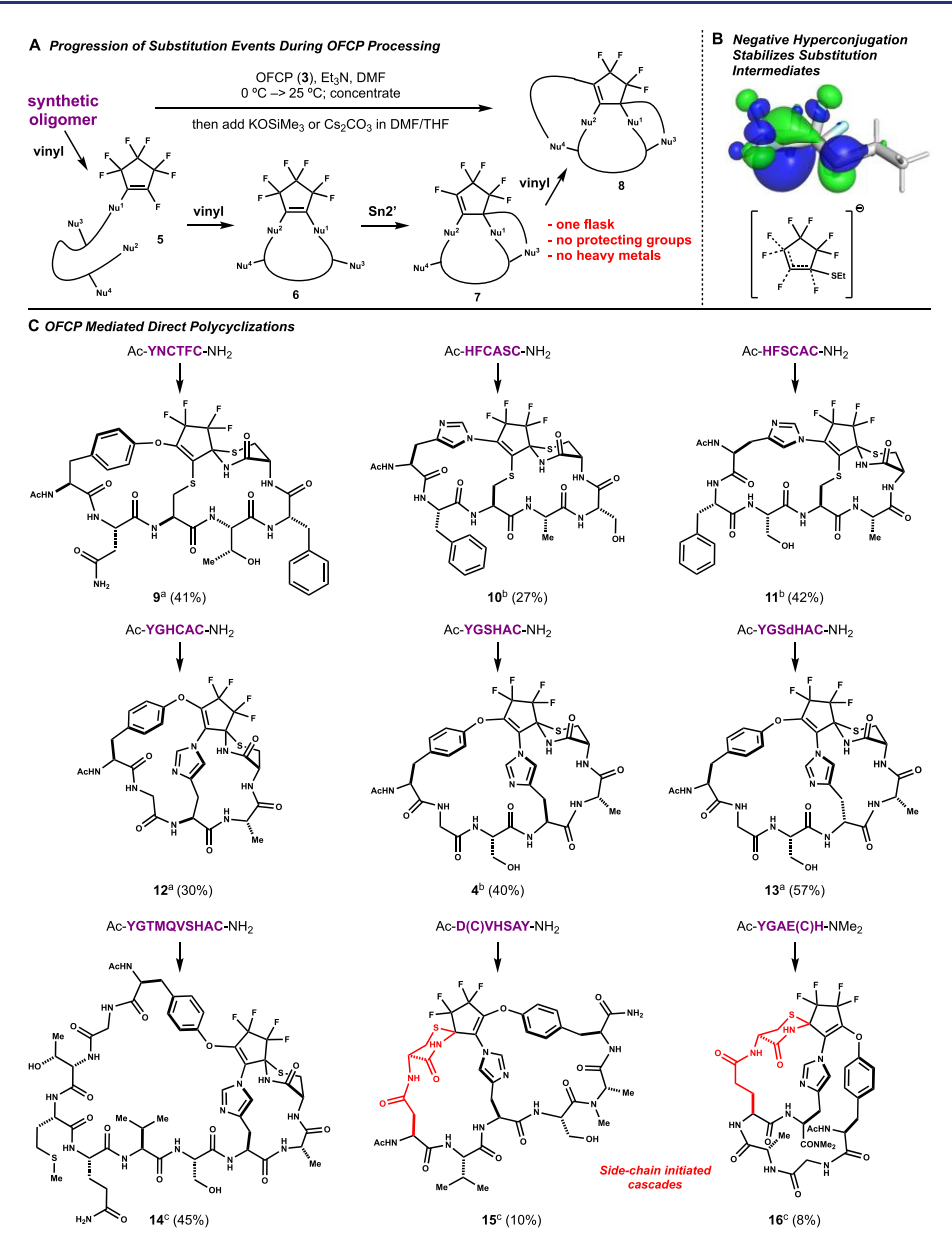


Figure 2. Direct macrobicyclization of linear unprotected peptides. (A) Progression of substitution events during OFCP processing. (B) Negative hyperconjugation stabilizes substitution intermediates. Computational rendering of the delocalized HOMO present in the intermediate formed by the model reaction of ethyl mercaptide + OFCP (M06-2x-D3/def2TZVP). See the Supporting Information (SI) for details. (C) OFCP-mediated direct polycyclizations. Linear peptides were synthesized on a solid phase as N-terminal acetamides and cleaved as primary C-terminal carboxamides. Yields reflect preparative HPLC isolation (C18 SunFire, using 0.1% TFA in $H_2O/MeCN$) wherein all histidine-derived products were isolated as TFA salts. Reagent and conditions: (a) OFCP (1.5 equiv), $E_{13}N$ (2.5 equiv), DMF (5.0 mM), 0 °C, 30 min; conc. then $E_{13}CO_{13}CO_{13}CO_{14}CO_{15}CO_$

decomposed at pH 10.0 and reacted readily with NCS (see the SI for details).

The reactivity of intermediate vinyl fluorides 7 provides options to form a second large ring using molecular inserts. This markedly expands the diversity of possible outcomes. In these experiments (Figure 4A), initial OFCP-mediated macrocyclizations and base-induced spirocyclizations occur in one flask as before. The incipient spirocyclic vinyl fluorides are then captured in situ with a nucleophile that can be subsequently activated as an electrophile. For example, treating Ac-YACFAC-NH $_2$ with 1.5 equiv OFCP (Et $_3$ N, DMF) forms a macrocycle at 0 °C (Figure 4B). Subsequent exposure to KOSiMe $_3$ generates a spirocyclic vinyl fluoride that is

intercepted in situ with hydroxymethylated thiazole thione 29 to afford 30 in good yield. The strong nucleophilicity of the exocyclic sulfur atom in 29 permits biomolecular substitution to outcompete internal macrocyclization of the tyrosyl phenol in this system. Warming a MeNO $_2$ solution of 30 containing 7.5 vol % TFA ionizes the primary hydroxyl group and the incipient methyldene thiazolium cation captures the tethered phenol via C–C bonding to generate macrobicyclic structure 31 in good yield.

This alkylative macrocyclization is tolerant of varying ring sizes and substitution patterns. Reacting 4-mer Ac-YCAC-NH₂ with OFCP and **29** in the same process as above affords the macrobicycle **32** wherein each large ring contains one less

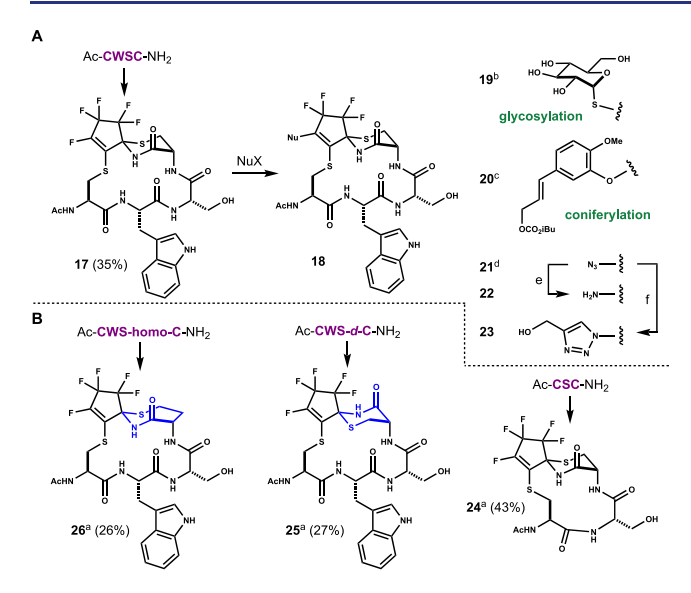


Figure 3. Intermediate spirocyclic vinyl fluorides can be isolated in isomeric forms and react efficiently with exogenous nucleophiles. (A) Bimolecular substitution reactions using compound 17. (B) Linear peptides were synthesized on the solid phase as N-terminal acetamides and cleaved as primary C-terminal carboxamides. Yields reflect preparative HPLC isolation (C18 SunFire, using 0.1% TFA in H2O/MeCN). Reagents and conditions: (a) OFCP (1.5 equiv), Et₃N (2.5 equiv), DMF (5.0 mM), 0 °C, 30 min; conc. then KOSiMe₃ (2.0 equiv), 1:4 DMF/THF (5.0 mM), 0 °C \rightarrow RT, 1 h, (>10:1 d.r.). (b) β -D-thioglucose sodium salt (1.0 equiv), DMF (50 mM), 0 °C, 1 h, >95%. (c) Coniferyl carbonate 33 (2.0 equiv), KOSiMe₃ (4.0 equiv), DMF (50 mM), 0 °C \rightarrow RT, 12 h, 53%. (d) NaN₃ (1.0 equiv), DMF (50 mM), 0 °C, 1 h, >95%. (e) H₂, Pd/C (10 wt %), EtOH, 35 °C, 12 h, 87%. (f) Propargyl alcohol (1.0 equiv), phenylenediamine (15 mol %), sodium ascorbate (10 mol %), CuSO₄·5H₂O (5 mol %), 2:3 $H_2O/tBuOH$ (0.2 M), 12 h, 75%.

amino acid residue. Replacing 29 with the coniferyl alcohol derivative 33 provides for further options. For example, treating Ac-YGHAC-NH2 with OFCP (Et3N, DMF) followed by an excess of Cs₂CO₃ generates a macrocyclic vinyl fluoride that reacts with the added 33 (2.0 equiv) to provide phenolic ether 34. Relative to 29, the capture rate by 33 is slower but the product is stable under the extended reaction conditions and is easily purified. When 34 is treated with Tf2NH in MeNO₂ at 25 °C for 1 h, preparative HPLC provides imidazolium-bridged macrobicyclic structure 35 in good yield. As we have shown previously, the cinnamyl cation, generated either as a solvated ion pair or in a metal-stabilized form, is adept at large ring formations. When Ac-WCASC-NH₂ is treated successively with OFCP and 33 as before and the resultant product is ionized with Sc(OTf)₃ in MeNO₂, the novel indole-linked macrobicycle 36 is produced.

Internal cinnamylation engages the otherwise unreactive (toward OFCP) tryptophan side chain in C-C bond formation.

The side chains of Asp and Glu were also potential sites for ring closures (Figure 4C). However, free carboxylate groups caused OFCP reactions to be chaotic and low yielding. Bode had developed a cyano sulfurylide masked form of Asp (D*) to avoid aspartimide forming truncations during SPPS. We synthesized monomer 37 and its new one carbon homolog 38. Each proved to be an excellent surrogate for Asp and Glu, respectively, during peptide synthesis and OFCP processing. For example, Ac-D*GSFAC-NH₂ reacts successively with

OFCP and Cs₂CO₃ to give a spirocyclic vinyl fluoride that is captured in situ with commercial cysteamine to form the adduct 39 (>10:1 d.r.). It is not necessary to isolate this species. Rather, mild oxidative hydrolysis of the cyano sulfurylide (NCS, CH₃CN/pH 4.5 acetate buffer, 25 °C) provides the corresponding carboxylic acid in high yield. Lactamization of the incipient amino acid then affords the macrobicyclic compound 40 in 30% overall yield from the starting peptide. Product 40 contains a bridging serine residue. Identical OFCP processing of the cyano sulfurylide residue containing peptides tolerates variations in peripheral functionality (see 41, 44, and 45) as well as threonine bridging (42 and 46). The synthesis of the imidazolium salt-bridged macrobicycle 43 directly from Ac-D*PNHFTC-NH2 highlights the complex-forming potential of the methods. Replacing cysteamine with 2-mercaptoethanol or thiazole thione 29 permits the EDC-mediated synthesis of macrolactones 47-49. Structures of this kind are prototypes for a new class of hybrid cyclodepsipeptides.

Cyclic peptides and peptidomimetics are potential ligands for protein surfaces involved in protein-protein interactions (PPIs).²⁴ The majority of characterized protein-protein interactions (PPIs) are mediated by nonhelical, nonstrand surface loops.²⁵ Kritzer and co-workers analyzed more than 1400 contiguous "hot" loops mediating PPIs in the Protein Data Bank and found the large majority clustered into just 11 backbone structural types. 26 Because spectroscopic data indicated that the thiazaspirodecenone scaffolded double looped structures in Figure 2C were conformationally well defined, we hypothesized that selective mimics of Kritzer's "hot" loops might be devised by varying ring sizes on either side of the bridging residue.²⁷ To probe this idea, we analyzed a hypothetical library of macrobicycles resulting from OFCP processing of Ac-X- $(Ala)_m$ -Y- $(Ala)_n$ -Cys-NH₂ sequences: where X = Cys, His, and Tyr, Y = Cys and His and m, n = 1-5. Each of these 150 structures was geometry-optimized using molecular force fields and low energy conformations were identified using a Monte Carlo search algorithm (see the SI). Conformers within 5 kcal/mol of the calculated minimum for each library member were overlaid onto a representative of the 11 Kritzer loop types using the PyMOL superposition function.²⁸ The conformer that aligned best in each case was assigned a MatchAlign score. These were then normalized relative to loop self-superimposed maximal values to yield "percent similarity" scores for each loop type. This method to evaluate structural mimicry permits meaningful comparisons across the macrobicycle and representative loop size variations.

Library members that best mimic each representative loop type are plotted along the diagonal (top right to bottom left) in the heat map shown in Figure 5. This core data set identifies close mimics (percent similarity > 75%) for six of the eleven major PPI-mediating loop types. Of these six, three appear quite selective, despite the analysis lacking side chain annotations. Interestingly, the data show that mimicry can occur at the N-terminal loop (see 2WAM/H5H2C overlay), the C-terminal loop (see 2OL1/H1H5C overlay), or at the composite surface created at the double loop junction (see 3N3R/Y4C1C overlay). In general, the double-looped nature of OFCP-derived products allows one turn surface to be conformationally geared by small perturbations in the second. For example, the 4J07/H4H4C overlay has a similarity score of 79.8 while the closely related 4J07/H4H5C overlay has a similarity score of 8.6 (see the SI for further details).

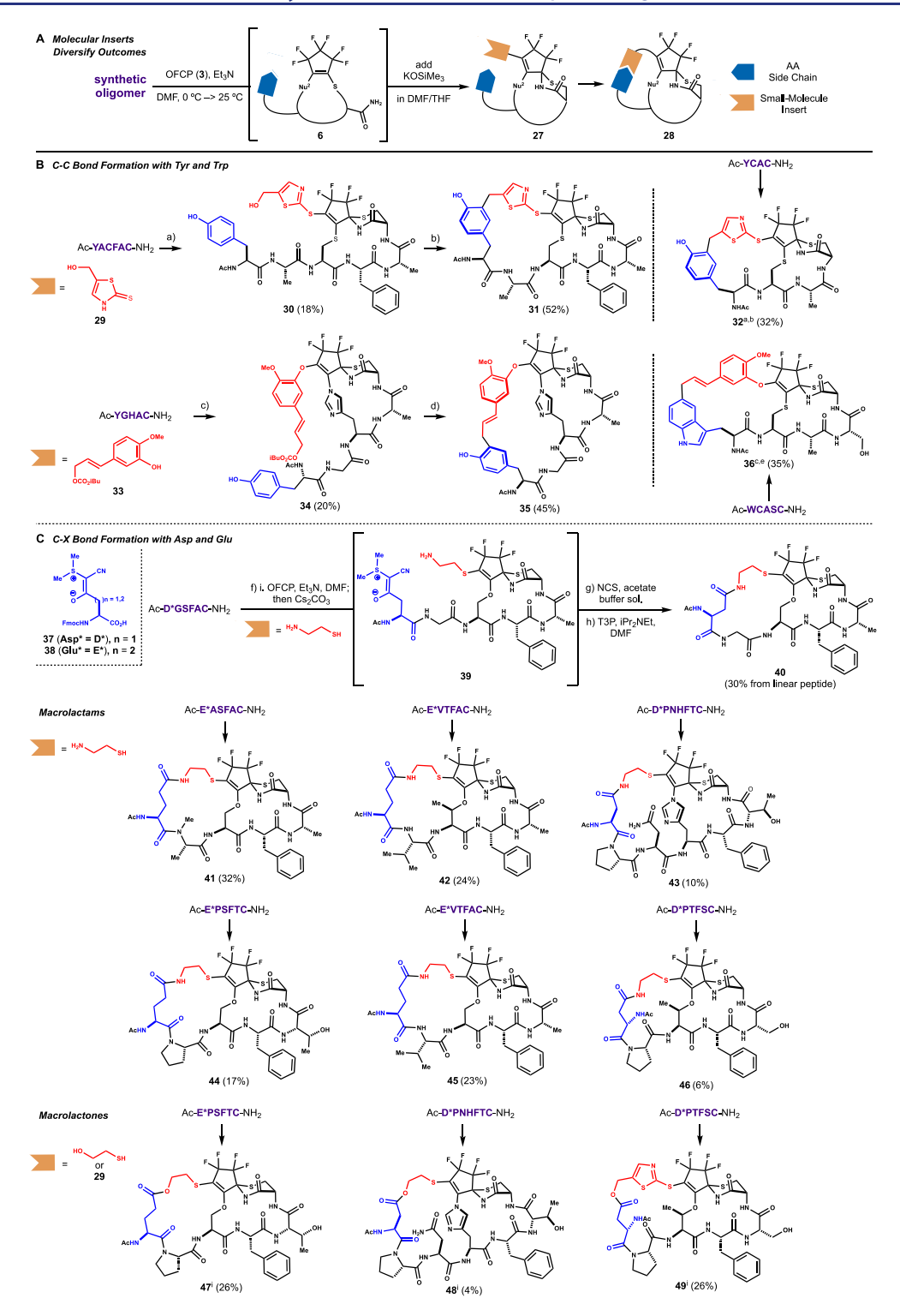


Figure 4. Synthesis of OFCP scaffolded macrobicyclic structures using small-molecule inserts. (A) Molecular inserts diversify outcomes. (B) C–C bond formation with Tyr and Trp. (C) C–X bond formation with Asp and Glu. Linear peptides were synthesized on a solid phase as N-terminal acetamides and cleaved as primary C-terminal carboxamides. Yields reflect preparative HPLC isolation (C18 SunFire, using 0.1% TFA in H₂O/MeCN) wherein all histidine-derived products were isolated as TFA salts. Yields shown for 40–49 refer to isolated yields from their respective linear oligomers. Reagents and conditions: (a) OFCP (1.5 equiv), Et₃N (2.5 equiv), DMF (10 mM), 0 °C, 30 min; conc. then KOSiMe₃ (3.5 equiv), thiazole 29 (1.2 equiv), 1:4 DMF/THF (30 mM), 0 °C – >RT, 3 h. (b) 7.5% TFA, MeNO₂ (5.0 mM), 80 °C, 12 h. (c) OFCP (1.5 equiv), NEt₃ (2.5 equiv), DMF (10 mM), 0 °C, 30 min; conc. then Cs₂CO₃ (6.0 equiv) 1:4 DMF/THF (30 mM) 0 °C, 1 h; then 33 (2.0 equiv), 0 °C – >RT, 48 h. (d) Tf₂NH (5.0 equiv), MeNO₂ (2.5 mM), RT, 1 h. (e) Sc(OTf)₃ (1.0 equiv), MeNO₂ (5.0 mM), RT, 1 h. (f) OFCP (1.5 equiv), NEt₃ (2.5 equiv), DMF (10 mM), 0 °C, 30 min; conc. then Cs₂CO₃ (5.0 equiv), 1:4 DMF/THF (30 mM), 0 °C, 1 h; then cysteamine, 2-mercaptoethanol, or 29 (1.2 equiv), 0 °C, 1 h. (g) NCS (1.5–3.0 equiv), 2:8 MeCN:NaOAc/AcOH (acetate buffer, pH 4.5) (1.0 mM), RT, 1 h. (h) Propanephosphonic acid anhydride (T3P) (1.5 equiv), iPr₂NEt (3.5 equiv), DMF (5.0 mM), 0 °C, 1 h. (i) Macrolactonization done using EDC·HCl (3.0 equiv), HOBt (2.0 equiv), Et₃N (5.0 equiv), DMF (5.0 mM), 0 °C – >RT, 44–64 h.

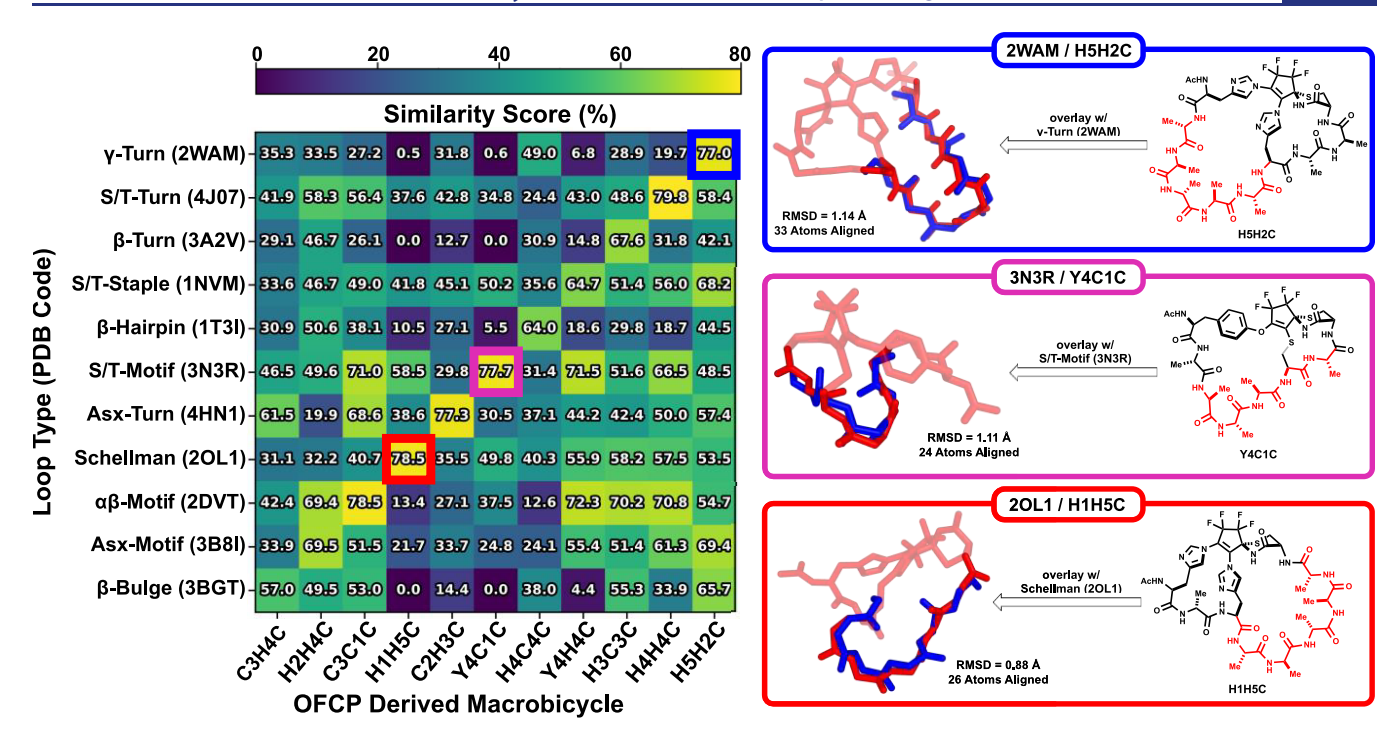


Figure 5. "Hot" loop backbone mimicry within a library of computed OFCP-derived poly-A macrobicycles. The heat map showing percent similarity scores between select OFCP-derived macrobicycles (*x*-axis) and various representative loop types (*y*-axis). Data along the diagonal (top right to bottom left) shows those macrobicycles which best structurally mimics each loop type. OFCP-processed macrobicycles are named based on the amino acid sequence of the peptide from which they were derived with letters corresponding to one letter amino acid abbreviations and numbers representing the number of intervening L-alanine residues between nucleophilic residues (see the SI for details). Reaction schemes to synthesize CXCXC- and HXHXC-derived macrobicycles are described in the SI. Each of the 150 OFCP-derived macrobicycles used in this study were geometry-optimized using molecular force fields and low energy conformations were identified using a Monte Carlo search algorithm (see the SI for details). Low energy conformers of each library member were overlaid onto a representative of the 11 Kritzer loop types using the PyMOL superposition function. The resulting generated MatchAlign scores were normalized relative to loop self-superimposed maximal values to yield "similarity scores". OFCP-derived macrobicycles demonstrate good loop mimicry utilizing their N-terminal loop (2WAM/H5H2C), C-terminal loop (20L1/H1H5C), as well as the composite surface created at the double loop junction (3N3R/Y4C1C) of the macrobicycle.

Computed backbone overlays generate hypotheses that can be validated in future experiments. The utility of these experiments will be broader if the macrocyclic compounds are membrane-permeant. Intracellular PPIs are particularly challenging to target with peptidic structures. Cyclic peptides having mw > 1 kDa are rarely taken up passively into cells.²⁹ Below 1 kDa, numerous factors must be considered. The fluorinated polycycles generated in this study are new chemotypes that have not been evaluated for permeability in any format. OFCP-derived macrocycles were analyzed in PAMPAs. Averaged data are plotted in Figure 6. Nearly 30% of the molecules tested showed $P_{\rm app} > 1.0 \times 10^{-6}$ cm/s, a "significant" permeability benchmark recently advocated by Baker and co-workers in studies of computationally designed peptidyl macrocycles. Notably, $P_{\rm app}$ measured for several compounds approached that of diclofenac and chloramphenicol—low molecular weight, orally bioavailable drugs used as permeability standards. Both mono and bimacrocyclic structures were among the most permeable (see Figure 6). In general, macrobicyclic products from Figure 4C show greater passive membrane permeability than their seco precursors. The imidazole-bridged macrobicycle 13 has mass = 804 Da, eight H-bond donors, and a calculated tPSA = 249 A², yet it is one of the most permeable compounds tested. Calculated low energy conformations of 13 (free base) in a low dielectric field appear to be stabilized by transannular hydrogen bonding in both large rings (shown in Figure 6). Low energy

conformers of the double-looped structure 15 are also calculated to be structured by internal hydrogen bonding, involving both the bridging imidazole and peripheral functional groups. "Chameleonic" conformational behavior that can transiently shield the polar surface area is thought to be a contributing factor for passive permeability observed in other "beyond rule of 5" macrocycles.³¹ However, experimental studies on larger compound sets will be needed to define parameters, including internal hydrogen bonding and peripheral fluorination, most correlated with passive membrane permeability in these systems.

CONCLUSIONS

In summary, relative rate-controlled polysubstitution cascades using perfluorocycloalkenes is a new methodology to rapidly generate complex fluorinated composite macrocycles. OFCP can directly polycyclize linear peptide sequences using native functionality, or fluorospiroheterocyclic intermediates can be intercepted with exogenous nucleophiles. The latter tactic can generate a range of molecular hybrids composed of peptides, sugars, lipids, and heterocyclic components. The platform can create both single- and double-looped macrocycles in multiple stereoisomeric forms. Subsets of these molecules will have low energy conformers that shield the polar surface area through intramolecular hydrogen bonding, a behavior that may correlate with passive membrane permeability. Ongoing studies are focused on OFCP-mediated polycyclizations that

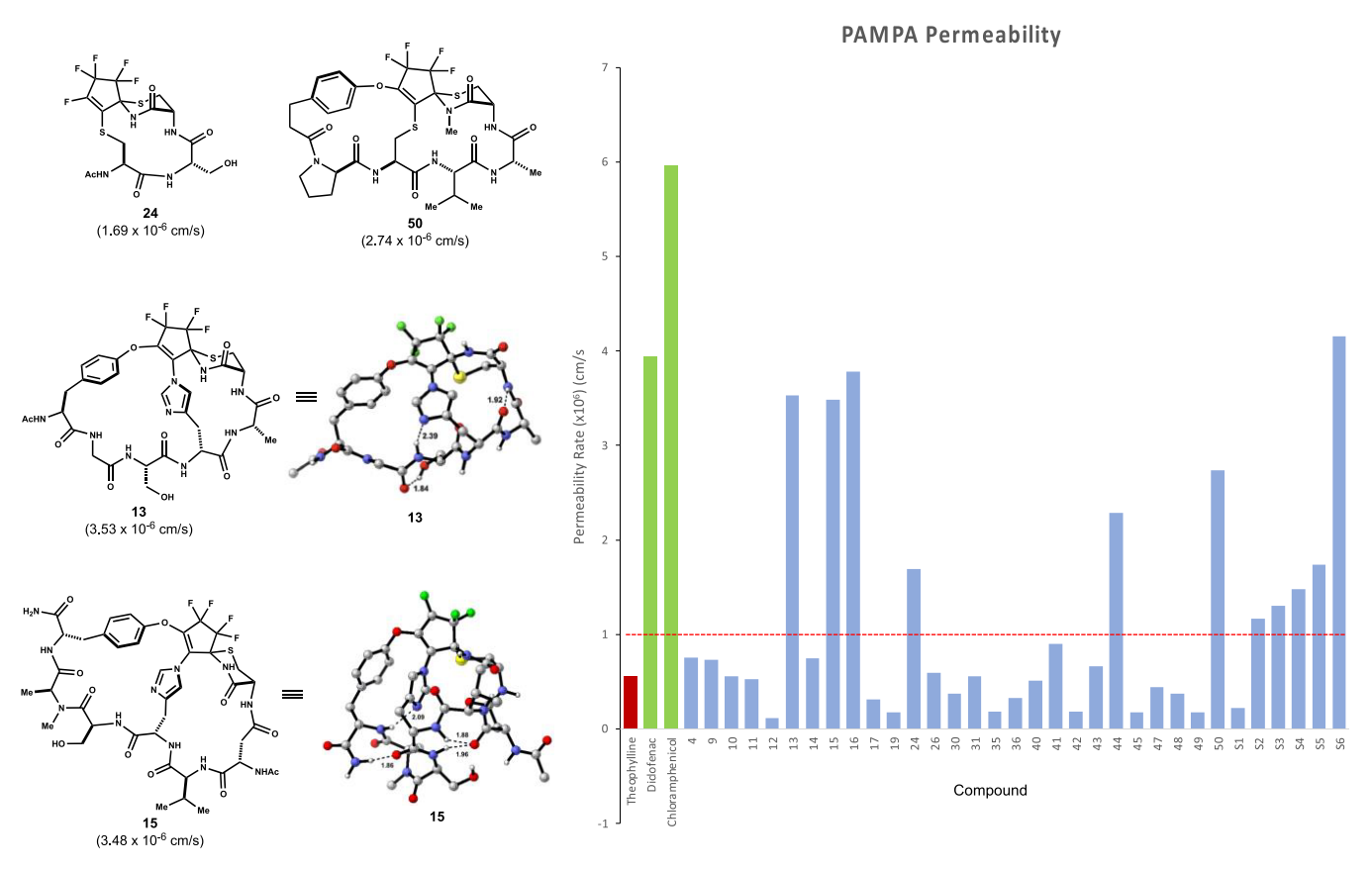


Figure 6. Evaluation of passive membrane permeability In vitro using parallel artificial membrane permeability assay (PAMPA). The bar graph shows averaged data from two independent experiments, each performed in a technical replicate in a 96-well format (UV—vis detection, see the SI for details). Theophylline, diclofenac, and chloramphenicol are low, medium, and high permeability standards, respectively. See the SI for a complete listing of molecules tested. PAMPA analyses of linear peptide precursors were complicated by their insolubility in assay buffer. Calculated low energy conformers of 13 and 15 were rendered using CYLview and annotated with intramolecular hydrogen bonds (bond lengths in angstroms) identified by Schrodinger Maestro MacroModel (see the SI for details).

generate fluorinated molecular probes for chemical biology research, new classes of glycopeptide conjugates, novel fluorinated antimicrobials and molecular "glues", as well as stable shape mimics of diverse loop structures mediating intracellular PPIs.³²

ASSOCIATED CONTENT

Supporting Information

The Supporting Information is available free of charge at https://pubs.acs.org/doi/10.1021/jacs.3c03071.

Experimental procedures, spectroscopic data (¹H NMR, ¹³C NMR, 2D NMR, variable-temperature NMR, HRMS, structural assignments, and X-ray), PAMPA data, and computational data (PDF)

■ AUTHOR INFORMATION

Corresponding Author

Patrick G. Harran – Department of Chemistry and Biochemistry, University of California, Los Angeles, Los Angeles, California 90095, United States; oorcid.org/ 0000-0001-8748-5167; Email: harran@chem.ucla.edu

Authors

Angel Mendoza — Department of Chemistry and Biochemistry, University of California, Los Angeles, Los Angeles, California 90095, United States; Occid.org/0009-0000-2435-5584 Salvador J. Bernardino – Department of Chemistry and Biochemistry, University of California, Los Angeles, Los Angeles, California 90095, United States

Morris J. Dweck – Department of Chemistry and Biochemistry, University of California, Los Angeles, Los Angeles, California 90095, United States; ⊚ orcid.org/ 0000-0003-2163-1904

Isabel Valencia — Departamento de Química Orgánica y Química Inorgánica, Universidad de Alcalá, Alcalá de Henares 28805, Spain

Declan Evans – Department of Chemistry and Biochemistry, University of California, Los Angeles, Los Angeles, California 90095, United States

Haowen Tian – Department of Chemistry and Biochemistry, University of California, Los Angeles, Los Angeles, California 90095, United States

William Lee – Department of Chemistry and Biochemistry, University of California, Los Angeles, Los Angeles, California 90095, United States

Yu Li – Department of Chemistry and Biochemistry, University of California, Los Angeles, Los Angeles, California 90095, United States

Kendall N. Houk – Department of Chemistry and Biochemistry, University of California, Los Angeles, Los Angeles, California 90095, United States; orcid.org/ 0000-0002-8387-5261

Complete contact information is available at:

https://pubs.acs.org/10.1021/jacs.3c03071

Author Contributions

§A.M. and S.J.B. contributed equally to this work.

Notes

The authors declare the following competing financial interest(s): P.G.H., S.J.B., A.M., M.J.D. have filed a provisional patent application on OFCP-derived peptidic macrobicycles and related structures.

ACKNOWLEDGMENTS

We are grateful to Mr. Ta-Chung Ong (UCLA) for assistance with multidimensional NMR analyses. Funding provided by the Donald J. and Jane M. Cram Endowment (to P.G.H.), the NSF (CHE-2153972 to K.N.H.), the NIH grant (1S10OD028644 to UCLA), and major equipment grant NSF CHE-1048804 is acknowledged. A.M. acknowledges the Foote Family Fellowship and the NSF predoctoral fellowship (DGE-1650604). D.E. was supported by the UCLA NIH CBI training grant. A.M. and S.J.B. were recipients of UCLA Cota-Robles Fellowships. Visiting scholar I.V. acknowledges a mobility grant from the University of Alcalá.

REFERENCES

- (1) Nicolaou, K. C.; Chen, J. S. The art of total synthesis through cascade reactions. *Chem. Soc. Rev.* **2009**, *38*, 2993–3009.
- (2) Tietze, L. F. Domino Reactions in Organic Synthesis. *Chem. Rev.* **1996**, *96*, 115–136.
- (3) Zhao, H.; Negash, L.; Wei, Q.; LaCour, T. G.; Estill, S. J.; Capota, E.; Pieper, A. A.; Harran, P. G. Acid promoted cinnamyl ion mobility within peptide derived macrocycles. *J. Am. Chem. Soc.* **2008**, 130, 13864–13866.
- (4) Lawson, K. V.; Rose, T. E.; Harran, P. G. Synthesis of a designed sesquiterpenoid that forms useful composites with peptides and related oligomers. *Tetrahedron Lett.* **2011**, *52*, 653–654.
- (5) Lawson, K. V.; Rose, T. E.; Harran, P. G. Template-induced macrocycle diversity through large ring-forming alkylations of tryptophan. *Tetrahedron* **2013**, *69*, 7683–7691.
- (6) Lawson, K. V.; Rose, T. E.; Harran, P. G. Template-constrained macrocyclic peptides prepared from native, unprotected precursors. *Proc. Natl. Acad. Sci. U. S. A.* **2013**, *110*, E3753–E3760.
- (7) Rose, T. E.; Lawson, K. V.; Harran, P. G. Large ring-forming alkylations provide facile access to composite macrocycles. *Chem. Sci.* **2015**, *6*, 2219–2223.
- (8) Rose, T. E.; Curtin, B. C.; Lawson, K. V.; Simon, A.; Houk, K. N.; Harran, P. G. On the prevalence of bridged macrocyclic pyrroloindolines formed in regiodivergent alkylations of tryptophan. *Chem. Sci.* **2016**, *7*, 4158–4166.
- (9) Curtin, B. H.; Manoni, F.; Park, J.; Sisto, L. J.; Lam, Y.-h.; Gravel, M.; Roulston, A.; Harran, P. G. Assembly of Complex Macrocycles by Incrementally Amalgamating Unprotected Peptides with a Designed Four-Armed Insert. *J. Org. Chem.* **2018**, *83*, 3090–3108.
- (10) Sisto, L. J.; Harran, P. G. Sulfane transalkylations and metal catalyzed allylic substitutions for the synthesis of composite macrobicyclic peptides. *Tetrahedron Lett.* **2020**, *61*, No. 151986.
- (11) Sisto, L. J.; Harran, P. G. Syntheses of hybrid cyclopeptidyl [n]sulfanes by internal alkyl group exchange. *Tetrahedron Lett.* **2020**, *61*, No. 151985.
- (12) Goto, Y.; Suga, H. The RaPID Platform for the Discovery of Pseudo-Natural Macrocyclic Peptides. *Acc. Chem. Res.* **2021**, *54*, 3604–3617.
- (13) Spokoyny, A. M.; Zou, Y.; Ling, J. J.; Yu, H.; Lin, Y.-S.; Pentelute, B. L. A Perfluoroaryl-Cysteine SNAr Chemistry Approach to Unprotected Peptide Stapling. *J. Am. Chem. Soc.* **2013**, *135*, 5946–5949.

- (14) Zou, Y.; Spokoyny, A. M.; Zhang, C.; Simon, M. D.; Yu, H.; Lin, Y.-S.; Pentelute, B. L. Convergent diversity-oriented side-chain macrocyclization scan for unprotected polypeptides. *Org. Biol. Chem.* **2014**, *12*, 566–573.
- (15) Heinis, C.; Rutherford, T.; Freund, S.; Winter, G. Phage-encoded combinatorial chemical libraries based on bicyclic peptides. *Nat. Chem. Biol.* **2009**, *5*, 502–507.
- (16) Li, B.; Wan, Z.; Zheng, H.; Cai, S.; Tian, H.-W.; Tang, H.; Chu, X.; He, G.; Guo, D.-S.; Xue, X.-S.; Chen, G. Construction of Complex Macromulticyclic Peptides via Stitching with Formaldehyde and Guanidine. *J. Am. Chem. Soc.* **2022**, *144*, 10080–10090.
- (17) Saha, I.; Dang, E. K.; Svatunek, D.; Houk, K. N.; Harran, P. G. Computational generation of an annotated gigalibrary of synthesizable, composite peptidic macrocycles. *Proc. Natl. Acad. Sci. U. S. A.* **2020**, *117*, 24679–24690.
- (18) Sanger, F. The free amino groups of insulin. *Biochem. J.* **1945**, 39, 507–515.
- (19) Garg, S.; Twamley, B.; Zeng, Z.; Shreeve, J. M. Azoles as Reactive Nucleophiles with Cyclic Perfluoroalkenes. *Eur. J. Chem.* **2009**, *15*, 10554–10562.
- (20) Tsunemi, T.; Bernardino, S. J.; Mendoza, A.; Jones, C. G.; Harran, P. G. Syntheses of Atypically Fluorinated Peptidyl Macrocycles through Sequential Vinylic Substitutions. *Angew. Chem., Int. Ed.* **2020**, *59*, *674*–*678*.
- (21) Baron, A.; Blériot, Y.; Sollogoub, M.; Vauzeilles, B. Phenylenediamine catalysis of "click glycosylations" in water: practical and direct access to unprotected neoglycoconjugates. *Org. Biomol. Chem.* **2008**, *6*, 1898–1901.
- (22) Saulnier, M. G.; Dodier, M.; Frennesson, D. B.; Langley, D. R.; Vyas, D. M. Nucleophilic Capture of the Imino-Quinone Methide Type Intermediates Generated from 2-Aminothiazol-5-yl Carbinols. *Org. Lett.* **2009**, *11*, 5154–5157.
- (23) Neumann, K.; Farnung, J.; Baldauf, S.; Bode, J. W. Prevention of aspartimide formation during peptide synthesis using cyanosulfurylides as carboxylic acid-protecting groups. *Nat. Commun.* **2020**, *11*, 982.
- (24) Qian, Z.; Dougherty, P. G.; Pei, D. Targeting intracellular protein-protein interactions with cell-permeable cyclic peptides. *Curr. Opin. Chem. Biol.* **2017**, *38*, 80–86.
- (25) Guharoy, M.; Chakrabarti, P. Secondary structure based analysis and classification of biological interfaces: identification of binding motifs in protein-protein interactions. *Bioinformatics* **2007**, 23, 1909–1918.
- (26) Gavenonis, J.; Sheneman, B. A.; Siegert, T. R.; Eshelman, M. R.; Kritzer, J. A. Comprehensive analysis of loops at protein-protein interfaces for macrocycle design. *Nat. Chem. Biol.* **2014**, *10*, 716–722.
- (27) Guéret, S. M.; Thavam, S.; Carbajo, R. J.; Potowski, M.; Larsson, N.; Dahl, G.; Dellsén, A.; Grossmann, T. N.; Plowright, A. T.; Valeur, E.; Lemurrell, M.; Waldmann, H. Macrocyclic Modalities Combining Peptide Epitopes and Natural Product Fragments. *J. Am. Chem. Soc.* **2020**, *142*, 4904–4915.
- (28) The PyMOL Molecular Graphics System, Version 2.5.2; Schrödinger, LLC: New York, NY, 2015.
- (29) Matsson, P.; Kihlberg, J. How Big Is Too Big for Cell Permeability? J. Med. Chem. 2017, 60, 1662–1664.
- (30) Bhardwaj, G.; O'Connor, J.; Rettie, S.; Huang, Y.-H.; Ramelot, T. A.; Mulligan, V. K.; Alpkilic, G. G.; Palmer, J.; Bera, A. K.; Bick, M. J.; Piazza, M. D.; Li, X.; Hosseinzadeh, P.; Craven, T. W.; Tejero, R.; Lauko, A.; Choi, R.; Glynn, C.; Dong, L.; Griffin, R.; van Voorhis, W. C.; Rodriguez, J.; Stewart, L.; Montelione, G. T.; Craik, D.; Baker, D. Accurate de novo design of membrane-traversing macrocycles. *Cell* **2022**, *185*, 3520–3532.
- (31) Rossi Sebastiano, M.; Doak, B. C.; Backlund, M.; Poongavanam, V.; Over, B.; Ermondi, G.; Caron, G.; Matsson, P.; Kihlberg, J. Impact of Dynamically Exposed Polarity on Permeability and Solubility of Chameleonic Drugs Beyond the Rule of S. J. Med. Chem. 2018, 61, 4189–4202.
- (32) Schreiber, S. L. The Rise of Molecular Glues. *Cell* **2021**, *184*, 3–9.